ARTICLE

Reaction of C_2HCl_2+O_2: Combined TR-FTIR Spectroscopy and Electronic Structure†

Tian-cheng Xiang[a,b], Huan Wang[a], Kun-hui Liu[a], Hong-mei Zhao[a], Wei-qiang Wu[a], Hong-mei Su[a]*

a. State Key Laboratory of Molecular Reaction Dynamics, Beijing National Laboratory for Molecular Sciences, Institute of Chemistry, Chinese Academy of Sciences, Beijing 100190, China
b. College of Chemistry and Chemical Engineering, Xuchang University, Xuchang 461000, China

(Dated: Received on November 19, 2009; Accepted on November 26, 2009)

The product channels and mechanisms of the C_2HCl_2+O_2 reaction are investigated by step-scan time-resolved Fourier transform infrared emission spectroscopy and the G3MP2//B3LYP/6-311G(d,p) level of electronic structure calculations. Vibrationally excited products of HCl, CO, and CO_2 are observed in the IR emission spectra and the product vibrational state distribution are determined which shows that HCl and CO are vibrationally excited with the nascent average vibrational energy estimated to be 59.8 and 51.8 kJ/mol respectively. In combination with the G3MP2//B3LYP/6-311G(d,p) calculations, the reaction mechanisms have been characterized and the energetically favorable reaction pathways have been suggested.

Key words: TR-FTIR, G3MP2, Radical reaction, C_2HCl_2

I. INTRODUCTION

As an important organic chemical, trichloroethylene (TCE) is widely used in the industries, such as decontamination on the surface of metals [1], dry-cleaning, medicine manufacturing, and numerous other applications. It is also a very commonly used solvent for waxes, fats, resins, and oils. On the other hand, the inevitable release of the TCE to air, soil and water has made it one of the most populous pollutants, causing damage to crops and materials as well as having potential harmful effects on human health. Thus, TCE has drawn extensive research interests from the fields of photochemistry, atmospheric chemistry, and combustion chemistry [2−7]. C_2HCl_2 radicals could be released during the photoexcitation or pyrolysis of TCE. The reactions of such kind of radicals play critical roles in the chemical processes involving TCE.

Despite the importance of C_2HCl_2 radical studies on the reactions are rare. The photolysis of TCE and its photocatalytic oxidation reaction at 253.7 nm have been studied by Zuo *et al.* using the direct sampling mass spectrometry [8]. They observed CO_2, HCl, Cl_2, and $COCl_2$ as the products of photocatalytic oxidation reaction of TEC. But the reaction mechanisms, the elementary reactions accounting for the formation of these products, are unknown. Still, it is a good indication that the observed CO_2, HCl, Cl_2, and $COCl_2$ from the photocatalytic oxidation reaction of trichloroethylene might originate from the free radical reactions of C_2HCl_2 with O_2.

However, it has been lack of the knowledge on the product channels and mechanism of the elementary reaction of C_2HCl_2 with O_2 in the literature. In this work, we intend to study the C_2HCl_2+O_2 reaction comprehensively by combining the experimental measurements with the electronic structure calculations. The elementary reaction products are detected by means of step-scan time-resolved Fourier transform infrared emission (TR-FTIR) spectroscopy which is an effective technique probing multiple IR-active reaction products in real time due to its multiple advantage and nanosecond time resolution. Electronic structure calculations at the G3MP2//B3LYP/6-311G(d,p) level are performed to characterize the reaction mechanisms forming these products. By exploring the energies and geometries of the major intermediates and transition states along the potential energy surface, the minimum energy reaction paths are obtained. In combination with the experimental TR-FTIR spectroscopic detection of the reaction products, the elementary reaction channels and their formation mechanisms are characterized for the C_2HCl_2+O_2 reaction.

II. EXPERIMENTAL AND THEORETICAL METHODS

The step-scan TR-FTIR is an effective technique to acquire broad-band, time-resolved spectra of multiple products simultaneously. The title reaction products

†Part of the special issue for "the Chinese Chemical Society's 11th National Chemical Dynamics Symposium".
*Author to whom correspondence should be addressed. E-mail: hongmei@iccas.ac.cn

 ©2009 Chinese Physical Society

are monitored by step-scan TR-FTIR. The details of the setup have been described thoroughly in prior publications [9], and a brief introduction is presented here. The instrument consists of a Nicolet Nexus 870 step-scan FTIR spectrometer, Lambda Physik (LPX305i) excimer laser, and a pulse generator (Stanford Research DG535) to initiate the laser pulse and achieve synchronization of the laser with data collection. The internal 100 kHz 16-bit digitizer and external 100 MHz 14-bit GAGE 14100 digitizer could offer fast time resolution and a wide dynamic range as needed. The whole experiment is controlled by a personal computer. The detector used in this experiment is the liquid nitrogen cooled InSb detector.

Theoretically, all *ab initio* calculations are carried out using the Gaussian 03 program package [10]. The geometries of the reactants, products, various intermediates, and transition states are fully optimized using the hybrid density functional theory (DFT), Becke's three-parameter nonlocal exchange functional of Lee, Yang, Parr (B3LYP) [11] with 6-311G(d,p) basis set. Harmonic vibrational frequencies and then the zero-point energies (ZPE) are calculated at the same level with the optimized geometries. The reactants, products, and intermediates are characterized by all the real frequencies, whereas the transition states possess one and only one imaginary frequency. The intrinsic reaction coordinate (IRC) [12] calculations are carried out to confirm the transition state connecting the corresponding local minima at the B3LYP/6-311G(d,p) level. In order to obtain more reliable energies, the single-point energy calculations are performed at the second-order Moller-Plesset Gaussian-3 level of theory (G3MP2) using the B3LYP/6-311G(d,p) optimized geometries.

III. RESULTS AND DISCUSSION

A. Photolytic source of C_2HCl_2 radicals

C_2HCl_2 radicals were prepared by KrF laser photolysis of C_2HCl_3 at 248 nm. The laser intensity was controlled under 10^7 W cm^2 in order to avoid the existence of multi-photon processes. Even at a low power density, the one-photon photodissociation of C_2HCl_3 molecules might undergo two channels:

$$\begin{aligned} C_2HCl_3 &\rightarrow Cl + C_2HCl_2 \\ &\rightarrow HCl + C_2Cl_2 \end{aligned}$$

Fortunately, the photofragment HCl and C_2Cl_2 are unreactive stable molecules and not likely to react with O_2. The reactions of the Cl atom with O_2 are either endothermic or slightly exothermic and hence can be neglected. Therefore, all the co-existed photofragments Cl atoms, HCl molecules, and chlorinated acetylenes C_2Cl_2 are not likely to compete with the highly reactive C_2HCl_2 radicals in their reaction with O_2 molecules within the time scale of experimental measurements, *i.e.*, tens of μs. The photodissociation of C_2HCl_3 molecules provide a good source of C_2HCl_2 radicals for the study of its consecutive reaction with O_2 molecules.

Possibly, the photodissociation of the precursor C_2HCl_3 could give rise to three isomers of C_2HCl_2 radicals, *trans*-CHCl=CCl, *cis*-CHCl=CCl, and CH=CCl$_2$. The *cis*-CHCl=CCl is the most stable isomer (7.1 and 21.3 kJ/mol lower in energy than that of *trans*-CHCl=CCl and CH=CCl$_2$, respectively, according to the B3LYP/6-311G(d,p) calculations). Which is the most important species? UV absorption spectra measured by Berry show that chloroethylene C_2HCl_3 has two absorption bands in a region between 260 and 140 nm [13]. A broad absorption band at about 200 nm is assigned to the $\pi^* \leftarrow \pi$ transition. Both 193 and 248 nm excitation falls into this absorption band, corresponding to the $\pi^* \leftarrow \pi$ transition, and is expected to yield identical photofragments. Upon the 193 nm photolysis of the precursor C_2HCl_3, the *cis*-CHCl=CCl was observed as the major isomer of the fragment C_2HCl_2 radicals [14]. Besides, the most favorable decomposition reaction pathway of C_2HCl_3 was demonstrated to be Cl+*cis*-CHCl=CCl in another experiment [15]. Most recently Bylaska *et al.* calculated the cleavage of the R−Cl bonds of the polychlorinated ethylenes, including C_2Cl_4, C_2HCl_3, *trans*-1,2-$C_2H_2Cl_2$, *cis*-1,2,-$C_2H_2Cl_2$, 1,1-$C_2H_2Cl_2$, and C_2H_3Cl at the RHF-CCSD(T)/aug-cc-pVTZ//B3LYP/6-311++G(2d,2p) level [16]. The calculation suggested that the reduction of C_2HCl_3 tends to show selectivity toward the formation of *cis*-1,2-C_2HCl_2 over the formation of *trans*-1,2-C_2HCl_2 and 1,1-C_2HCl_2 radicals. All of these experimental and theoretical references indicated that the photodissociation of the precursor C_2HCl_3 should yield dominantly the radical species of the *cis*-CHCl=CCl rather than the other two isomers, *trans*-CHCl=CCl, and CH=CCl$_2$. Even though the much less radical species *trans*-CHCl=CCl and CH=CCl$_2$ may be involved in the reaction with O_2, they are expected to lead to identical products to that of the *cis*-CHCl=CCl since these radical species are basically the isomers of one radical C_2HCl_2. Therefore, we only perform theoretical calculations of the reaction of the major isomer, *cis*-CHCl=CCl with O_2.

B. Identification of the reaction products

The TR-FTIR emission spectroscopy can probe vibrationally excited species formed from either the photolysis of precursor or the products of the consecutive radical reactions. In the reference experiment when pure precursor C_2HCl_3 was photolyzed, only very weak HCl emission signal was observed, providing a slight background for the further detection of the reaction of *cis*-CHCl=CCl with O_2. When the mixture of 13 Pa of C_2HCl_3 and 110 Pa of O_2 was irradiated by 248 nm laser, strong IR emission signals from the reaction products of C_2HCl_2+O_2 were detected. After subtracted from the pure photodissociation background, the TR-

DOI:10.1088/1674-0068/22/06/673-680 ©2009 Chinese Physical Society

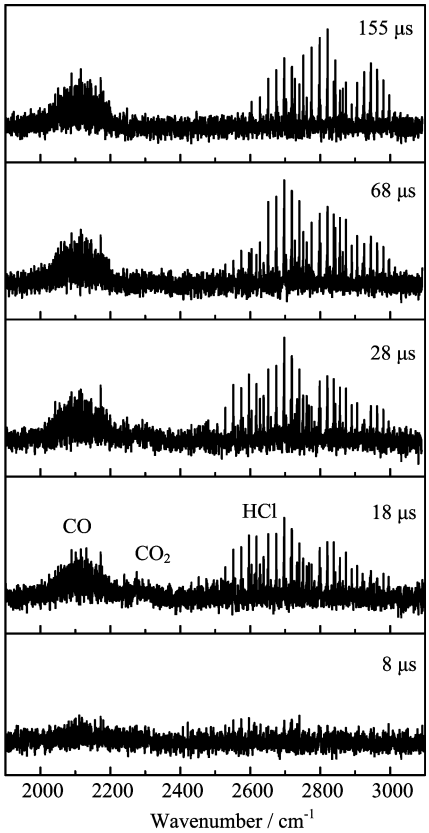

FIG. 1 Product TR-FTIR emission spectra from the reaction of $C_2HCl_2+O_2$ taken at typical reaction times from 8 μs to 155 μs after initiation of the reaction by 248 nm laser photolysis. The spectral were collected using the InSb detector with the spectral resolution of 0.5 cm^{-1}.

FTIR emission spectra for the $C_2HCl_2+O_2$ reaction products were obtained and the spectra at typical reaction times from 8 μs to 155 μs are displayed in Fig.1.

Three IR emission bands can be clearly identified from 2000 cm^{-1} to 3000 cm^{-1}. The strong rotationally resolved emission bands spreading 2000 cm^{-1} to 2200 cm^{-1} are due to the rovibrational lines of the $\Delta v=-1$ transitions of vibrationally excited CO. Next to CO, a very weak emission band spanning from 2200 and 2350 cm^{-1} can hardly be rotationally resolved which should be ascribed to the polyatomic CO_2 (v_1, v_2, v_3)→(v_1, v_2, v_{3-1}) according to its spectral position. The third emission band from 2500 cm^{-1} to 3100 cm^{-1} can be assigned to the rovibrational transitions of HCl ($v\rightarrow v-1$) based on its rotational structure and vibrational frequency. From the transient IR emission spectra, three reaction products HCl, CO, and CO_2 can be identified.

C. Vibrational state distribution of the products CO and HCl

A spectral fitting has been performed for the rotationally resolved CO and HCl emission bands using the spectral constants of these two molecules and a nonlinear least-squares fitting program which has been described in detail elsewhere [17]. Representative fitting results shown in Fig.2 and Fig.3, demonstrate further that these two bands are ascribed to CO and HCl molecules. The best fitted rotational temperature is 300 K, indicating that the rotational excitation has been thermalized. About 150 collisions take place within 28 μs at a total pressure of 120 Pa, which is sufficient to quench the rotational excitation to room temperature but not to alter the vibrational excitation much. For the 28 μs CO emission band, the best fitted vibrational populations of CO are 1.00±0.015, 0.49±0.008, 0.28±0.006, 0.14±0.005,

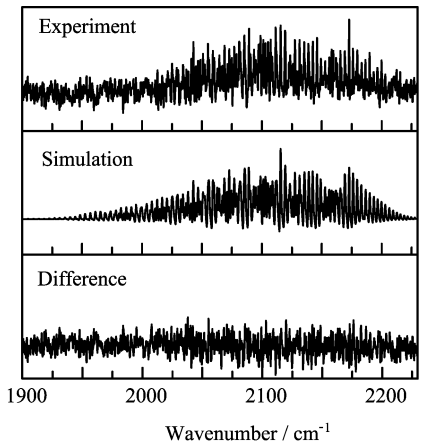

FIG. 2 Experimental and spectral fitting result for the IR emission bands of the products CO at the reaction times of 28 μs.

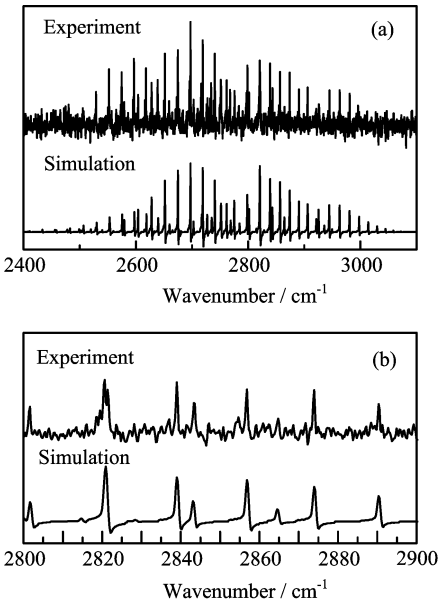

FIG. 3 (a) Experimental and spectral fitting result for the IR emission bands of the product HCl at 28 μs. (b) The spectral details range from 2800 cm^{-1} to 2900 cm^{-1}.

DOI:10.1088/1674-0068/22/06/673-680 ©2009 Chinese Physical Society

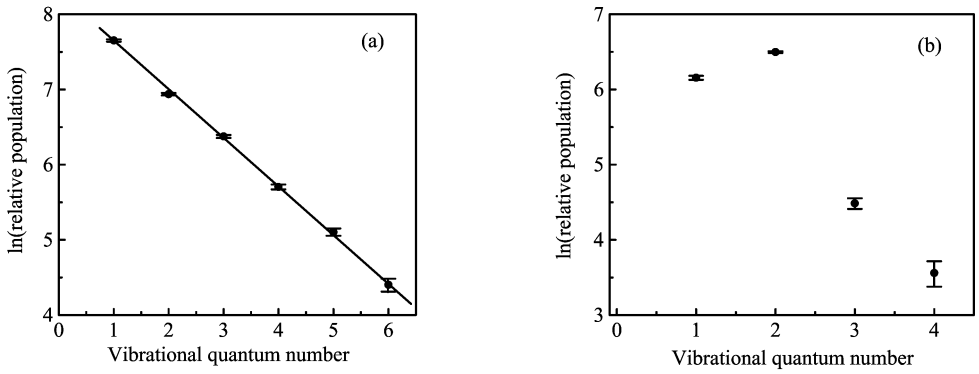

FIG. 4 Representative plots of the vibrational distribution of the product (a) CO and (b) HCl at 28 μs. The straight lines are the best fit of the data to a Boltzmann distribution with a temperature of 4900±100 K for CO.

0.08±0.004, 0.04±0.003 for the vibrational levels of v=1−6 indicating that the band is comprised of six Δv=−1 progressions of rovibrational transitions. For the 28 μs HCl emission band, the best fitted vibrational populations of HCl are 0.70±0.019, 1.00±0.011, 0.14±0.009, 0.05±0.009 for the vibrational levels of v=1−4. The IR emission band of HCl is therefore attributed to four Δv=−1 progressions of rovibrational transitions. To test the reliability of the spectral fitting program, the vibrational populations of HCl are also calculated manually. Each vibration-rotational line in the P-branch is integrated and divided by its respective Einstein coefficient to yield relative population of $P_v(J)$ and the sum of $P_v(J)$ for every J level gives the total population for the vibrational level of v. The populations obtained in this way agrees well with those acquired from the spectral fitting, indicating that the nonlinear least-squares fitting program can provide reliable vibrational state distributions.

As shown in Fig.4, the vibrational populations of CO derived from the spectral fitting are found to obey the Boltzmann distribution with a Boltzmann vibrational temperature of $T_{\rm vib}$=4900±100 K, while another product HCl exhibits an inverted vibrational population at v=2. The average vibrational energy can be calculated from the normalized vibrational population N_v using the equation of

$$\langle E_{\rm vib}\rangle = \sum_{v=1}^{v_{\rm max}} N_v E_v \qquad (1)$$

The corresponding average vibrational energy of CO and HCl at 28 μs is calculated respectively to be 50.2 and 59.4 kJ/mol. Likewise, the average vibrational energies of CO and HCl at various reaction times are obtained and listed in Table I. For both products, the average vibrational energy does not alter much with time, indicating that there is no significant vibrational relaxation in the reaction system within the time scale of experimental measurements, *i.e.*, tens of μs. The nascent vibrational energy of CO and HCl can then be estimated to be close to 51.8 and 59.8 kJ/mol respectively. For the polyatomic product CO_2, the intensity of the emission spectra is fairly weak and could not be fitted.

TABLE I Average vibrational energy of CO and HCl at different reaction times t.

t/μs	E_v(CO)/(kJ/mol)	E_v(HCl)/(kJ/mol)
11	51.8	59.8
18	50.2	60.6
28	50.2	59.4
38	49.7	58.5
52	51.4	55.6

D. Reaction mechanisms

The vibrationally excited products CO, HCl, and CO_2 from the reaction of C_2HCl_2 with O_2 have been observed in the time-resolved IR emission spectra. These products may arise from the following energetically accessible channels:

$$\begin{aligned} C_2HCl_2 + O_2 &\rightarrow CHCl_2 + CO_2 \\ &\quad \Delta H = -535.0\ \text{kJ/mol} \\ &\rightarrow HCl + CO + ClCO \\ &\quad \Delta H = -459.4\ \text{kJ/mol} \\ &\rightarrow HClCO + ClCO \\ &\quad \Delta H = -359.1\ \text{kJ/mol} \\ &\rightarrow CCl + HCl + CO_2 \\ &\quad \Delta H = -277.6\ \text{kJ/mol} \end{aligned}$$

What are the feasible channels and what are the detailed reaction mechanisms accounting for the formation of these products? Electronic structure calculations at the level of G3MP2//B3LYP/6-311G(d,p) are performed to answer this question. Geometries of the reactants, products, various intermediates, and transition states are optimized at the B3LYP/6-311G(d,p) level and their single-point energies are refined at

DOI:10.1088/1674-0068/22/06/673-680 ©2009 Chinese Physical Society

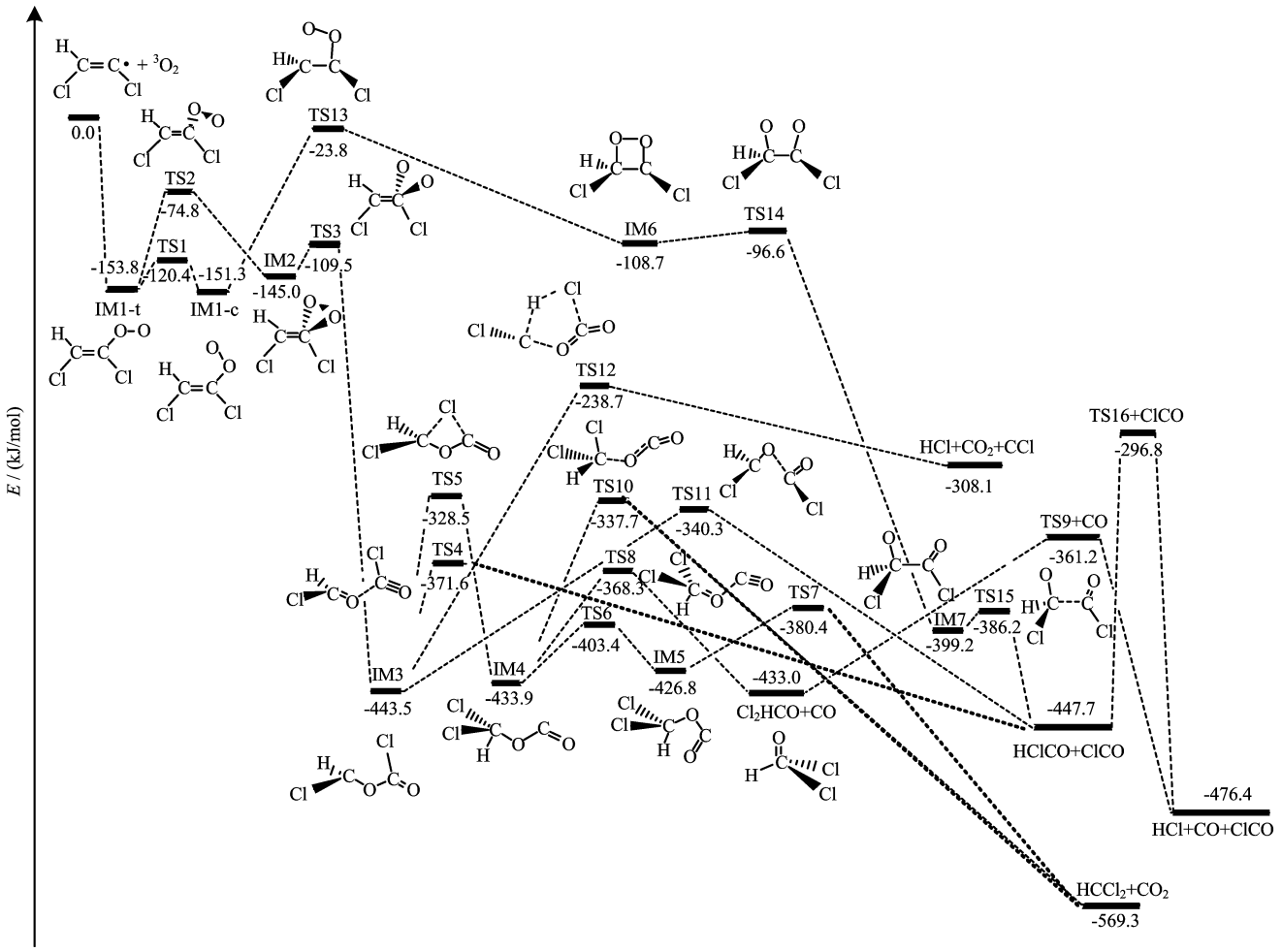

FIG. 5 The potential energy profiles of the reaction obtained at the G3MP2//B3LYP/6-311G(d,p) level.

the G3MP2/6-311G(d,p) level using the B3LYP/6-311G(d,p) optimized geometries. Profiles of the potential energy surface of the reaction pathways are shown in Fig.5. The optimized geometries of the various reactants, intermediate, transition states, and products are summarized in Fig.6.

The reaction starts with the addition of O_2 to the C_2HCl_2 radical forming a peroxy intermediate C_2HCl_2-O-O without any barrier. Two isomers of $C_2HCl_2O_2$, *trans* (IM1-t) and *cis* (IM1-c) conformations, are optimized depending on the different orientation of the initial attack of O_2. The energy of IM1-t and IM1-c is 153.8 and 151.3 kJ/mol lower than that of the reactants, respectively. IM1-t and IM1-c can isomerize to each other through a transition state (TS1). In view of the bond lengths, the C−C bond of the peroxy intermediate IM1 keeps the double bond feature. The O−O bond is stretched to the single bond in IM1 and the bond length is 1.320 Å in IM1-t and 1.322 Å in IM1-c. Therefore, the radical site shifts from C_2HCl_2 to the terminal O atom of $C_2HCl_2O_2$ after initial addition.

There are two reaction pathways starting from IM1. The energetically favorable one is the formation of the three-member-ring intermediate IM2, while the other pathway forming the four-member-ring intermediate IM6 is much less competitive because it requires surmounting much high barrier. Although it appears that the three-member-ring structure should have stronger strain and be less stable than four-member-ring structure, the calculation shows that IM2 (−145.0 kJ/mol) is more stable than IM6 (−108.7 kJ/mol).

1. The lowest-energy reaction channel

The reaction pathway forming the three-member-ring IM2 is more energetically favorable compared to the four-member-ring route by surmounting a low barrier of 79.0 kJ/mol. From IM1-t to IM2, the O3−O4 bond length is stretched from 1.320 Å to 1.508 Å (see Fig.6). Thus, the O3−O4 bond in the three-member-ring IM2 is significantly weakened. Subsequently, the breaking of O3−O4 bond of IM2 happens via TS3 with a barrier of 35.5 kJ/mol. It is interesting to note that O4 atom of IM2 tends to attack C1 via a three-member-

DOI:10.1088/1674-0068/22/06/673-680 ©2009 Chinese Physical Society

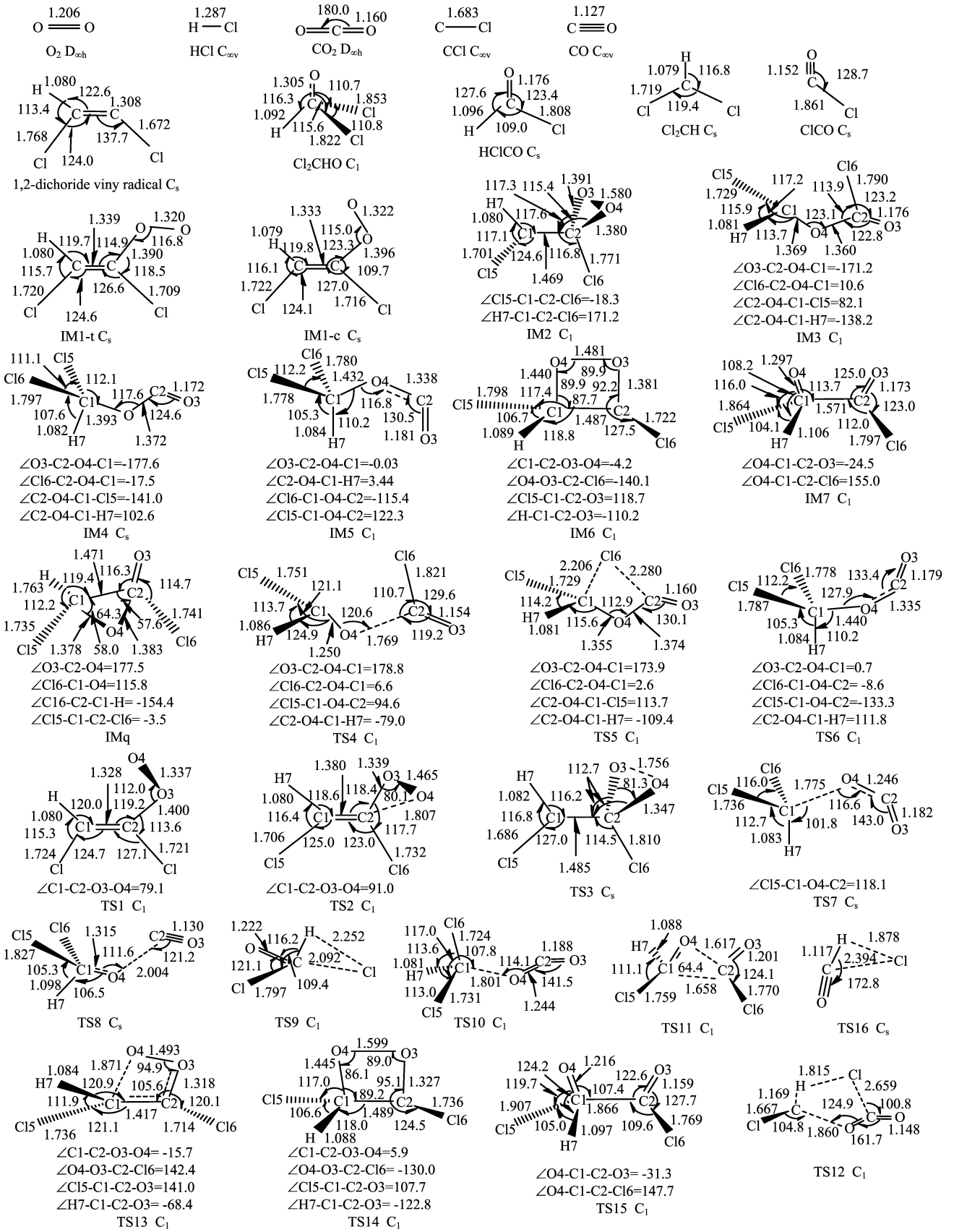

FIG. 6 The optimized geometries of the various reactants intermediates, transition states, and products at the B3LYP/6-311G(d,p) level. Bond lengths are in Å, angles and dihedral angles are in (°).

DOI:10.1088/1674-0068/22/06/673-680 ©2009 Chinese Physical Society

ring intermediate IMq, and then the O4 atom of IMq inserts into the C1−C2 bond. The C1−O4−C2−O4 backbone is then formed in IM3. IMq is a transient, quasi-stable species and only exists at the lower levels of theory (*e.g.* HF/6-311G*). It disappears at B3LYP/6-311G(d,p) level. It can be seen from Fig.5, the energy of IM3 is 443.5 kJ/mol lower than that of the reactant. Thus, a large amount of available energy is deposited into IM3, and many product channels are open starting from IM3. The dominant product channel through IM3 is the formation of HClCO+ClCO via a transition state TS4 and a barrier of 71.9 kJ/mol, corresponding to the lowest-energy reaction path for the reaction of C_2HCl_2 with O_2. The observed final product CO could be released from the further dissociation of ClCO. Another product from this channel, HClCO turns out to be quite stable and is not expected to undergo secondary dissociation to HCl+CO because of the high barrier of 150.9 kJ/mol as shown in Fig.6.

2. Reaction channel forming the product CO_2

There are also other pathways through IM3. The Cl6 atom of IM3 could migrate from one carbon atom C2 to the other one C1 by overcoming a barrier of 115.0 kJ/mol via TS5 and then IM4 is formed. The energy difference between IM3 and IM4 is only 9.6 kJ/mol. IM4 undergoes subsequent isomerization and decomposition forming a variety of final products. The feasible reaction channel through IM4 is the torsion of C2O3 group leading to the formation of IM5 via TS6. The barrier of TS6 is 30.5 kJ/mol. Subsequent decomposition of IM5 forms $HCCl_2+CO_2$. This should be the most feasible reaction pathway accounting for the formation of the product CO_2 which has also been detected in the TR-FTIR emission spectra.

3. Reaction channel forming the product HCl

IM4 could also dissociate directly to Cl_2HCO+CO overcoming the barrier of 65.6 kJ/mol via TS8, which is 35.1 kJ/mol higher than that of TS6. The product CO was released. Then Cl_2HCO decomposes to HCl and ClCO via TS9. This should be the most likely pathway yielding the product HCl which has been observed experimentally. It is noteworthy here that the transition state TS9 leading to the product HCl has a H−Cl bond length (2.252 Å) significantly larger than that of the free HCl bond length (1.287 Å) which should result in the highly vibrationally excited product HCl. In fact, our experiment has shown that HCl exhibits an inverted vibrational state distribution. This agreement suggests from another aspect that IM4 →TS8→Cl_2HCO+CO→TS9+CO→HCl+CO+ClCO should be the most probable reaction pathway leading to the product HCl. The whole reaction pathway is rate-limited by the barrier of 115.0 kJ/mol from IM3 to IM4. Although HCl may also arise from the further dissociation of HClCO via TS16, the process is always rate-limited by a high barrier of 150.9 kJ/mol no matter how easily HClCO can be formed through the lowest-energy reaction path of IM3→TS4→HClCO+ClCO, and thus is much less competitive.

There are also other product channels forming HClCO+ClCO, HCl+CO+ClCO, $HCCl_2+CO_2$, and $HCl+CO_2+CCl$, but are much less favorable because of much higher energy barrier. They are not discussed in detail.

Overall, the above calculations indicate that the reaction pathways leading to HClCO+ClCO, $HCCl_2+CO_2$, and HCl+CO+ClCO should be the major product channels. The dominant reaction pathway is $C_2HCl_2+O_2$→TS2→IM2→TS3→IM3→TS4→HClCO+ClCO. There are also another two favorable pathways. One is the pathway leading to the product CO_2: $C_2HCl_2+O_2$→TS2→IM2→TS3→IM3→TS5→IM4→TS6→IM5→TS7→$HCCl_2+CO_2$. The other is the pathway yielding HCl and CO: $C_2HCl_2+O_2$→TS2→IM2→TS3→IM3→TS5→IM4→TS8→Cl_2HCO+CO→TS9+CO→HCl+CO+ClCO. The product CO may arise from the HCl+CO+ClCO channel or the further dissociation of the HClCO+ClCO channel.

IV. CONCLUSION

In summary, the products and mechanisms of the $C_2HCl_3+O_2$ reaction are investigated by step-scan time-resolved Fourier transform infrared emission spectroscopy and the G3MP2//B3LYP/6-311G(d,p) level of electronic structure calculations. Vibrationally excited products of HCl, CO, and CO_2 are observed in the IR emission spectra and the product vibrational state distribution are determined which shows that HCl and CO are vibrationally excited with the nascent average vibrational energy estimated to be 59.8 and 51.8 kJ/mol respectively. In combination with the G3MP2//B3LYP/6-311G(d,p) calculations, the reaction mechanisms have been characterized. The reaction pathways leading to HClCO+ClCO, $HCCl_2+CO_2$, and HCl+CO+ClCO are suggested to be energetically favorable. The lowest-energy reaction path corresponds to: $C_2HCl_2+O_2$→TS2→IM2 (peroxide C_2Cl_2−OO)→TS3→IM3 (three-member-ring COO intermediate)→TS4→HClCO+ClCO. These experimental and theoretical characterization of the $C_2HCl_3+O_2$ reaction can add knowledge to the elementary channels and mechanisms of this type of chlorinated hydrocarbon radicals that are heavily involved in various atmospheric and combustion processes.

V. ACKNOWLEDGMENTS

This work was supported by the National Natural Science Foundation of China (No.20733005,

DOI:10.1088/1674-0068/22/06/673-680 ©2009 Chinese Physical Society

No.20673126, and No.20973179), the National Basic Research Program of China (No.2007CB815200 and No.2007AA02Z116), and the Chinese Academy of Sciences.

[1] S. Y. Nishida, S. C. March, K. Nagano, M. A. Anderson, and K. Hori, J. Phys. Chem. **99**, 15814 (1995).
[2] R. J. Cvetanovic, J. Phys. Chem. Ref. Data **16**, 261 (1987).
[3] J. Hranisavljevic and A. Fontijn, J. Phys. Chem. **99**, 12809 (1995).
[4] P. M. Cometto, M. A. Teruel, R. A. Taccone, and S. I. Lane, J. Phys. Org. Chem. **18**, 142 (2005).
[5] Z. Jiang, P. H. Taylor, and B. Dellinger, J. Phys. Chem. **97**, 5050 (1993).
[6] R. Atkinson, D. L. Baulch, R. A. Cox, R. F. Hampson Jr., J. A. Kerr, and J. Troe, J. Phys. Chem. Ref. Data. **21**, 1125 (1992).
[7] M. A. Teruel, R. A. Taccone, and S. I. Lane, Int J. Chem. Kinet. **33**, 415 (2001).
[8] G. M. Zuo, Z. X. Cheng, M. Xu, and X. Q. Qiu, J. Photochem. Photobio. A: Chemistry, **161**, 51 (2003).
[9] T. C. Xiang, K. H. Liu, S. L. Zhao, H. M. Su, F. A. Kong, and B. S. Wang, J. Phys. Chem. A **111**, 9606 (2007).
[10] M. J. Frisch, G. W. Trucks, H. B. Schlegel, G. E. Scuseria, M. A. Robb, J. R. Cheeseman, J. A. Montgomery, T. Jr. Vreven, K. N. Kudin, J. C. Burant, J. M. Millam, S. S. Iyengar, J. Tomasi, V. Barone, B. Mennucci, M. Cossi, G. Scalmani, N. Rega, G. A. Petersson, H. Nakatsuji, M. Hada, M. Ehara, K. Toyota, R. Fukuda, J. Hasegawa, M. Ishida, T. Nakajima, Y. Honda, O. Kitao, H. Nakai, M. Klene, X. Li, J. E. Knox, H. P. Hratchian, J. B. Cross, V. Bakken, C. Adamo, J. Jaramillo, R. Gomperts, R. E. Stratmann, O. Yazyev, A. J. Austin, R. Cammi, C. Pomelli, J. W. Ochterski, P. Y. Ayala, K. Morokuma, G. A. Voth, P. Salvador, J. J. Dannenberg, V. G. Zakrzewski, S. Dapprich, A. D. Daniels, M. C. Strain, O. Farkas, D. K. Malick, A. D. Rabuck, K. Raghavachari, J. B. Foresman, J. V. Ortiz, Q. Cui, A. G. Baboul, S. Clifford, J. Cioslowski, B. B. Stefanov, G. Liu, A. Liashenko, P. Piskorz, I. Komaromi, R. L. Martin, D. J. Fox, T. Keith, M. A. Al-Laham, C. Y. Peng, A. Nanayakkara, M. Challacombe, P. M. W. Gill, B. Johnson, W. Chen, M. W. Wong, C. Gonzalez, and J. A. Pople, *Gaussian 03, revision B03*, Wallingford CT: Gaussian Inc., (2004).
[11] (a) A. D. Becke, J. Chem. Phys. **98**, 5648 (1993);
(b) C. Lee, W. Yang, and R. G. Parr, Phys. Rev. B **37**, 785 (1988).
[12] C. Gonzalez and H. B. Schlegel, J. Phys. Chem. **90**, 2154 (1989).
[13] M. J. Berry, J. Chem. Phys. **61**, 3114 (1974).
[14] H. P. Upadhyaya, A. Kumer, P. D. Naik, and A. V. Sapre, Chem. Phys. Lett. **321**, 411 (2000).
[15] K. Yokoyama, G. Fujisawa, and A. Yokoyama, J. Chem. Phys. **102**, 7902 (1995).
[16] E. J. Bylaska, M. Dupuis, and P. G. Tratnyek, J. Phys. Chem. A **112**, 3712 (2008).
[17] H. Su, J. Yang, Y. Ding, W. Feng, and F. Kong, Chem. Phys. Lett. **326**, 73 (2000).

DOI:10.1088/1674-0068/22/06/673-680 ©2009 Chinese Physical Society